Inventory:

Supplemental Figures S1-S6

Supplemental Experimental Procedures

Supplemental References

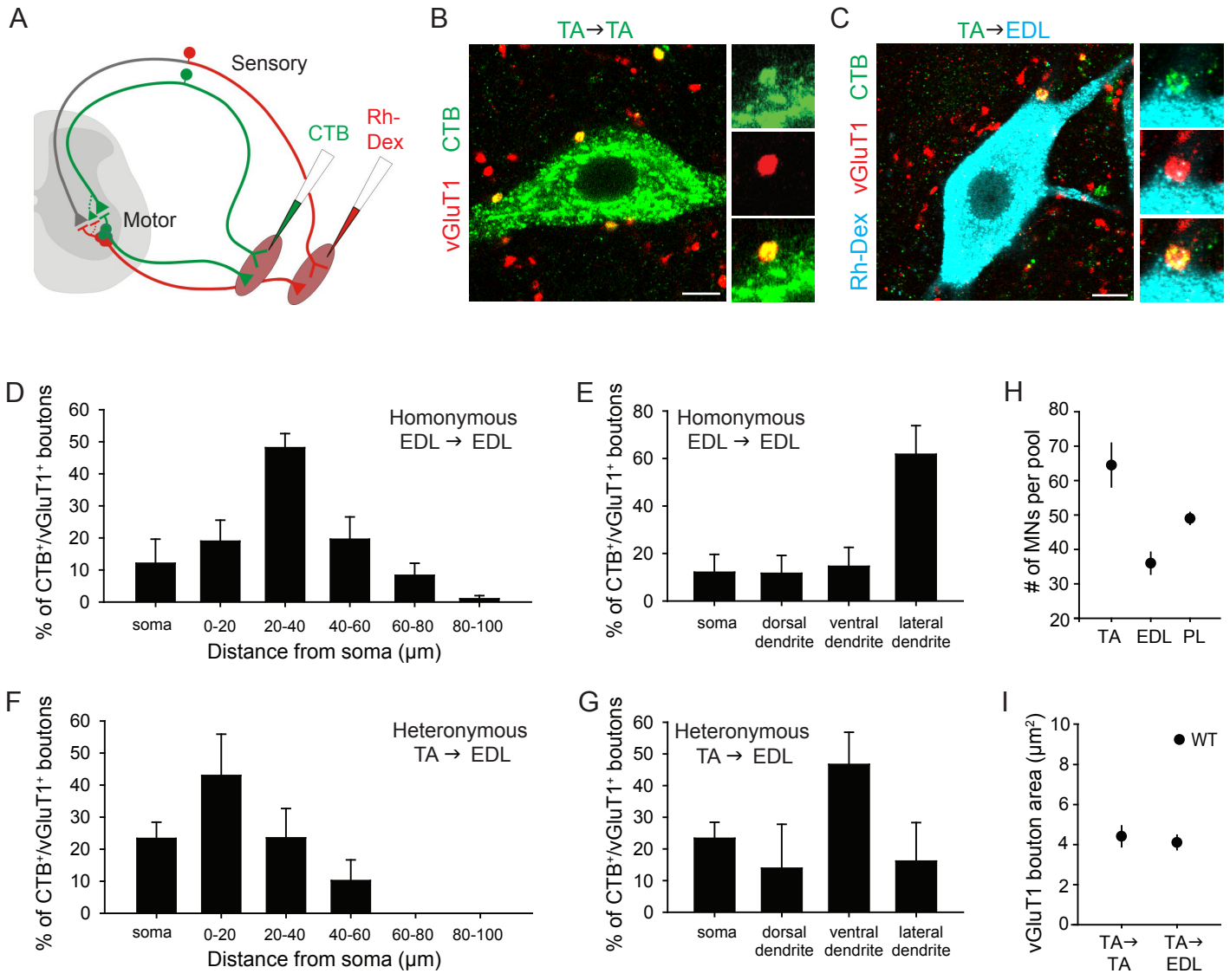

Figure S1, related to Figure 1. Distribution of Sensory-Motor Connections.

(A) Anatomical assay: after CTB and Rh-Dex tracer injection into different synergist muscles, CTB-labeled sensory terminals contact CTB-labeled homonymous or Rh-Dex-labeled heteronymous motor neurons.
(B) CTB-labeled vGluT1$^+$ TA sensory boutons on homonymous TA motor neuron.
(C) CTB-labeled vGluT1$^+$ TA sensory boutons on heteronymous EDL motor neuron. Rh-Dex was visualized with Rabbit anti-TMR antibody and Cy3 secondary, but rendered here in cyan for visualization purposes.
(D and E) Distribution of EDL sensory boutons on soma and proximal ~100 µm dendrite of EDL motor neurons in p21 wild-type mice (n = 5 mice).
(F and G) Distribution of TA sensory boutons on soma and proximal ~100 µm dendrite of EDL motor neurons in p21 wild-type mice (n = 3 mice).
(H) Average number of motor neurons counted per pool following CTB injection in p21 mice. TA: n = 4 mice. EDL: n = 4 mice. PL: n = 5 mice. Estimates are consistent with previous reports (Bácskai et al., 2014; McHanwell and Biscoe, 1981).
(I) Cross-sectional areas of TA sensory boutons on TA and EDL motor neurons in p21 wild-type mice (TA-TA: n = 27 boutons; 4 mice. TA-EDL: n = 26 boutons; 4 mice).
Scale bar represents 10 µm in (B) and (C). All data reported as mean ± SEM.

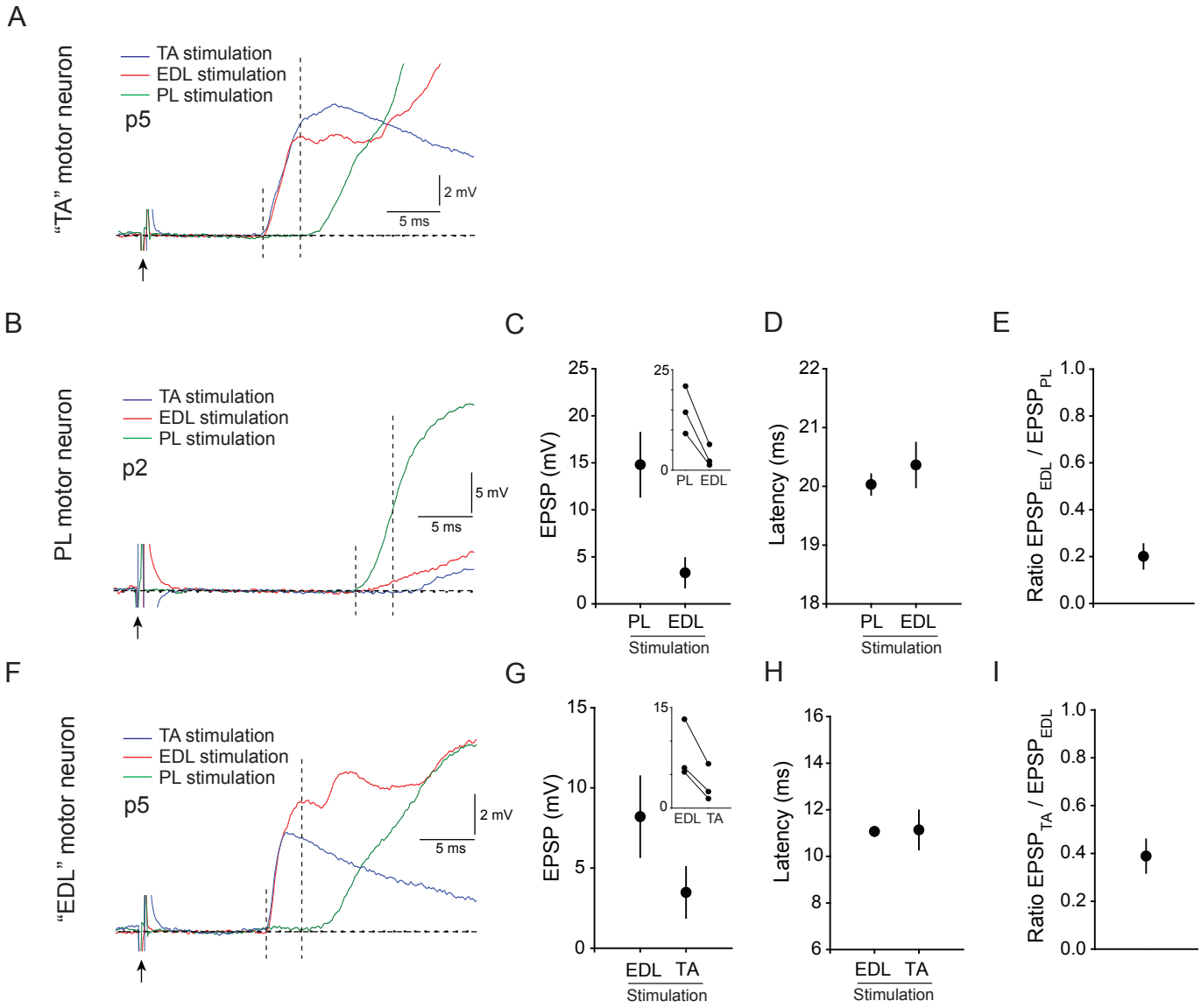

Figure S2, related to Figure 2. Additional Validation of Heteronymous Connections.

(A) Intracellularly recorded EPSPs in a single putative TA motor neuron upon stimulation of TA, EDL or PL muscle. Motor neuron was classified as TA based on absence of PL backfill and pattern of EPSP response. Traces averaged across 3 trials at 0.1 Hz.
(B) Intracellularly recorded EPSPs in a single retrogradely labeled PL motor neuron upon stimulation of PL, TA or EDL muscle. Single trials shown.
(C-E) Average EPSP amplitudes (C), latencies (D) and ratio of EPSP amplitudes (E) induced in PL motor neurons upon PL or EDL muscle stimulation (n = 3 MNs).
(F) Intracellularly recorded EPSPs in a single putative EDL motor neuron upon stimulation of EDL, TA or PL muscle. Traces averaged across 3 trials at 0.1 Hz.
(G-I) Average EPSP amplitudes (G), latencies (H) and ratio of EPSP amplitudes (I) induced in putative EDL motor neurons upon EDL or TA muscle stimulation (n = 3 MNs). Motor neurons were classified as EDL based on absence of TA or PL backfill and pattern of EPSP response.
All data reported as mean ± SEM.

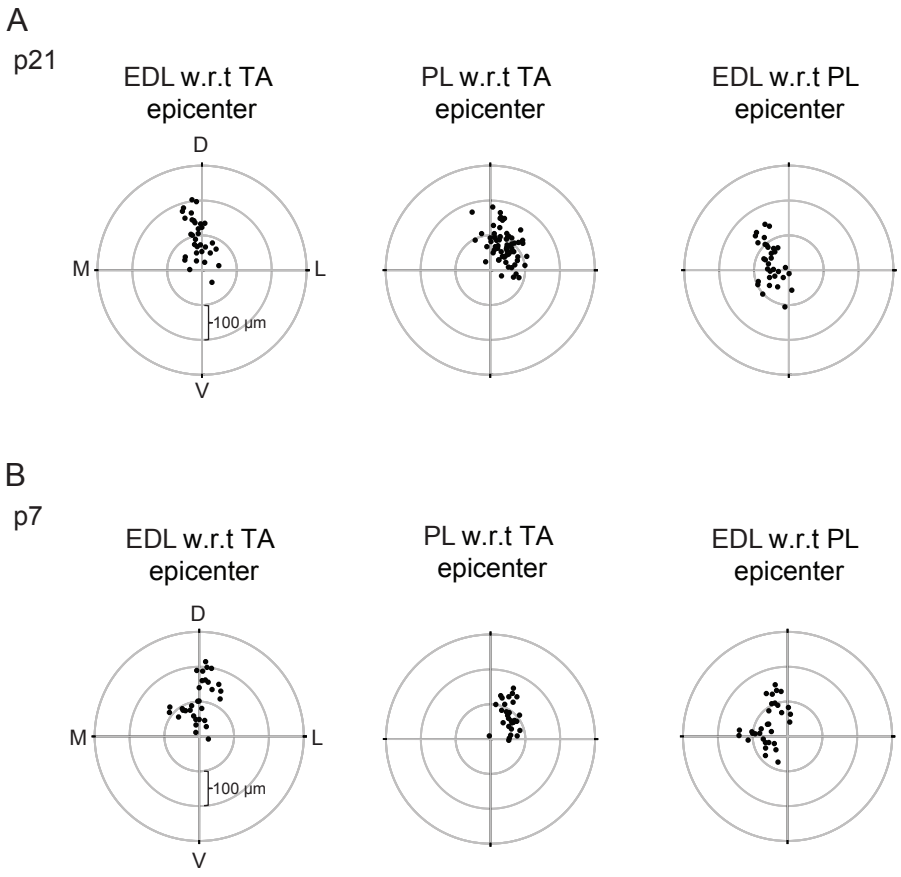

Figure S3, related to Figure 3. Spatial Relationships of Motor Neurons within the Anterolateral Crural Synergy Group.

(A and B) Individual cell body positions with respect to pool epicenter position at p21 (A) and p1-p7 (B). Each point represents one motor neuron with distance r and angle Ø with respect to the calculated epicenter position of each pool. D = Dorsal, V = Ventral, L = Lateral, and M = Medial.

For detailed methodology, see Supplemental Experimental Procedures.

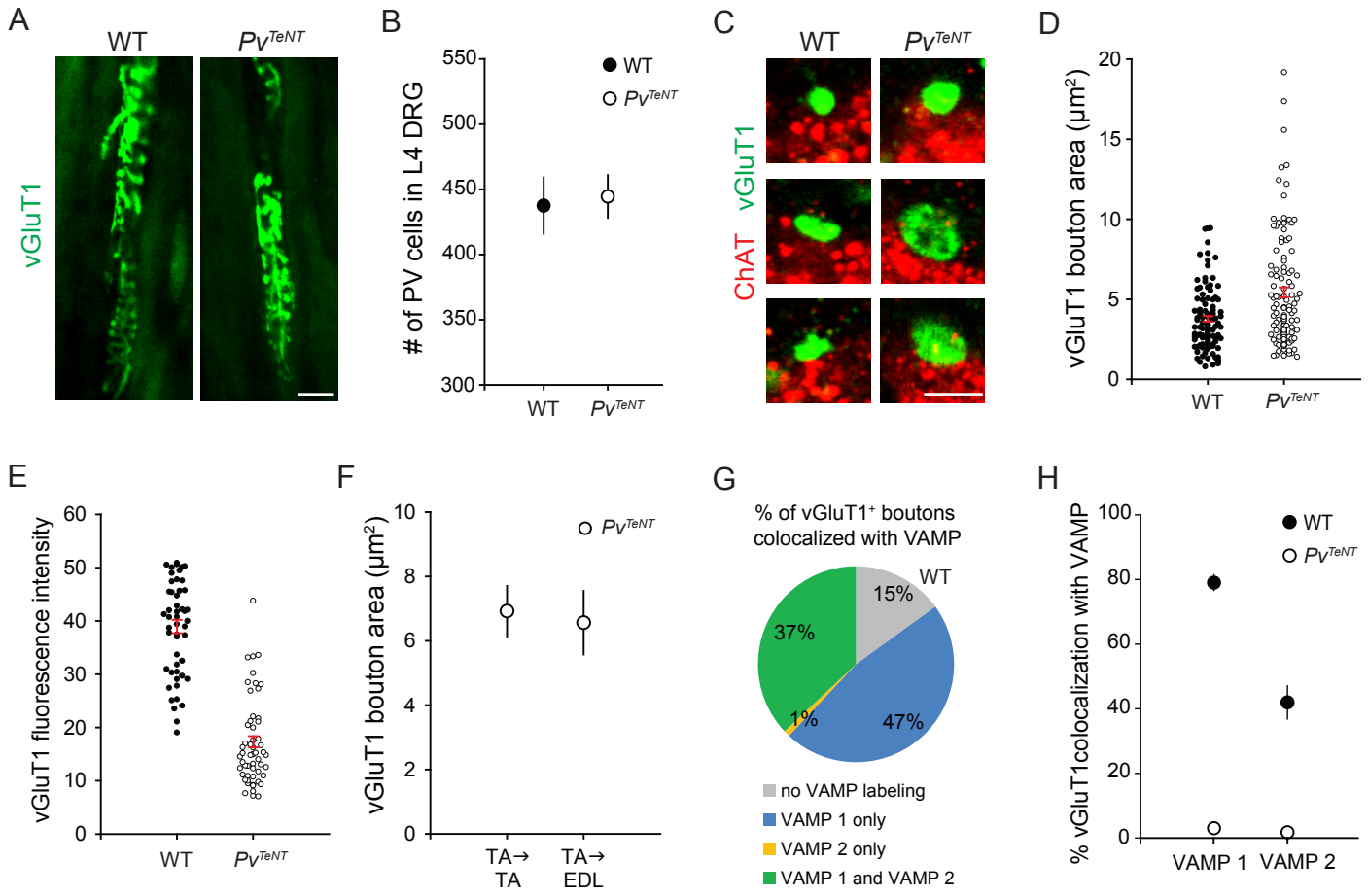

Figure S4, related to Figure 4. Preservation of Synaptic Morphology Following Tetanus Toxin Expression in Proprioceptors.

(A) vGluT1⁺ muscle spindle-associated sensory endings in tibialis anterior muscle at p18 in WT and *Pv*^{TeNT} mice.
(B) Number of Pv⁺ sensory neurons in L4 DRG at p18 in WT and *Pv*^{TeNT} mice (n = 4 mice).
(C) vGluT1⁺ boutons on ChAT⁺ motor neurons in p18 WT and *Pv*^{TeNT} mice.
(D) Cross-sectional areas of vGluT1⁺ boutons in p18 WT and *Pv*^{TeNT} mice. Outliers removed based on Grubbs outlier test ($p < 0.05$). Red lines indicate mean ± SEM. The difference in cross-sectional area is significant at $p < 0.001$ (Mann-Whitney Rank Sum Test. WT: n = 112 boutons; 3 mice. *Pv*^{TeNT}: n = 121 boutons; 3 mice).
(E) Mean pixel intensities of vGluT1⁺ boutons in p18 WT and *Pv*^{TeNT} mice (arbitrary fluorescence intensity units, using Adobe Photoshop histogram function). Outliers removed based on Grubbs outlier test ($p < 0.05$). Red lines indicate mean ± SEM. The difference in mean fluorescent intensity is significant at $p < 0.001$ (Student's t-test. WT: n = 50 boutons; 3 mice. *Pv*^{TeNT}: n = 57 boutons; 3 mice).
(F) Cross-sectional areas of TA sensory boutons on TA and EDL motor neurons in p18 *Pv*^{TeNT} mice (both TA-TA and TA-EDL: n = 31 boutons; 4 mice).
(G) Colocalization of VAMP1 and VAMP2 with vGluT1⁺ boutons in p21 WT mice (n = 100 boutons; 3 mice).
(H) Percentage of vGluT1⁺ boutons coexpressing VAMP 1 and VAMP 2 in p18 WT and *Pv*^{TeNT} mice. VAMP 1 colocalization with vGluT1 is reduced by 96% in *Pv*^{TeNT} mice ($p < 0.001$; Student's t-test. WT: n = 219 boutons; 3 mice. *Pv*^{TeNT}: n = 216 boutons; 3 mice). VAMP 2 colocalization with vGluT1 is reduced by 96% in *Pv*^{TeNT} mice ($p < 0.001$; Student's t-test. WT: n = 133 boutons; 3 mice. *Pv*^{TeNT}: n = 175 boutons; 3 mice).
Scale bars represent 50 µm in (A) and 5 µm in (C). All data reported as mean ± SEM.

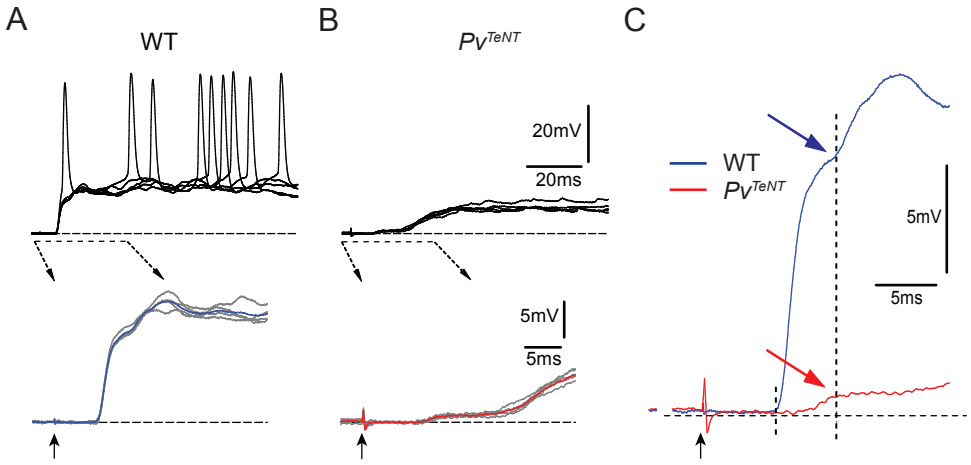

Figure S5, related to Figure 5. Subthreshold response of motor neuron under sensory silencing.

(A-B) Intracellular recordings from a L4 motor neuron following dorsal root L4 stimulation in p4 wild-type (A) and *Pv*^{TeNT} (B) mice. Four superimposed traces are shown. Traces are shown in a time expanded scale in bottom panels, with the average response shown in blue in (A) and red in (B) Black arrows indicate stimulus artifact.
(C) Superimposed average traces from (A) and (B). First dashed line indicates onset of EPSP response. Second dashed line indicates the maximum amplitude of the monosynaptic response, as determined at 3 ms after EPSP onset. Colored arrows indicate the amplitude of the monosynaptic EPSP measured.

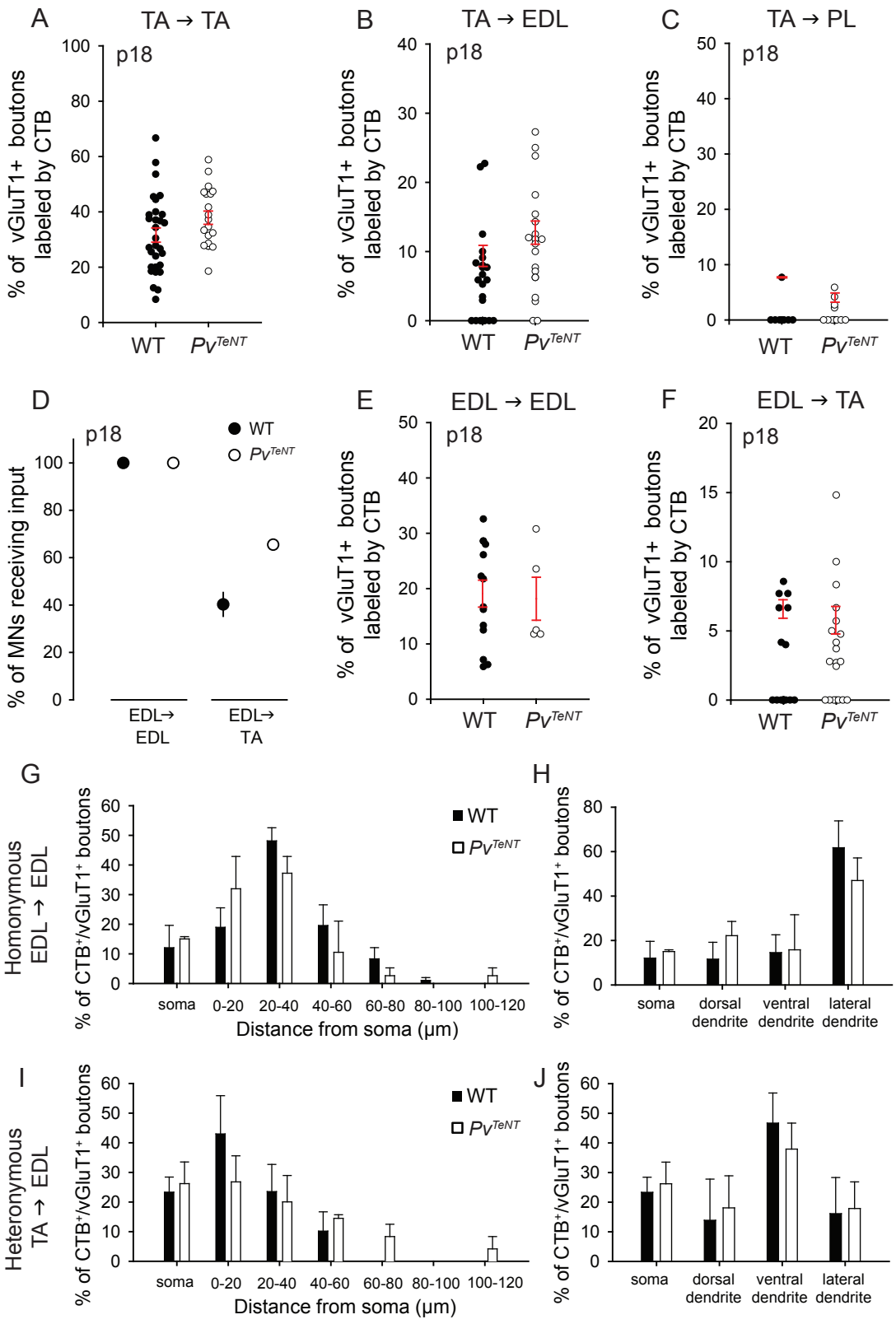
A
TA → TA
p18
% of vGluT1+ boutons labeled by CTB
WT
PvTeNT
B
TA → EDL
C
TA → PL
D
% of MNs receiving input
EDL→ EDL
EDL→ TA
E
EDL → EDL
F
EDL → TA
G
Homonymous EDL → EDL
% of CTB+/vGluT1+ boutons
soma
0-20
20-40
40-60
60-80
80-100
100-120
Distance from soma (µm)
H
dorsal dendrite
ventral dendrite
lateral dendrite
I
Heteronymous TA → EDL
J

Figure S6, related to Figure 6. Quantitation of Heteronymous Sensory-Motor Connectivity Following Tetanus Toxin Expression in Proprioceptors.

(A) Density of TA sensory input to TA motor neurons in p21 wild-type and p18 Pv^{TeNT} mice. Each point represents one motor neuron (WT: n = 30 MNs, as in Figure 1D. Pv^{TeNT}: n = 20 MNs). Red lines indicate mean ± SEM for motor neurons receiving TA input.
(B) Density of TA sensory input to EDL motor neurons in p21 wild-type and p18 Pv^{TeNT} mice (WT: n = 29 MNs, as in Figure 1D. Pv^{TeNT}: n = 20 MNs).
(C) Density of TA sensory input to PL motor neurons in p21 wild-type and p18 Pv^{TeNT} mice (WT: n = 31 MNs, as in Figure 1D. Pv^{TeNT}: n = 24 MNs).
(D) Percentage of EDL and TA motor neurons contacted by EDL sensory afferents in p21 WT and p18 Pv^{TeNT} mice. Difference in percentage of TA motor neurons receiving EDL input is significant at p = 0.03 (Student's t test; WT: n = 3 mice, as in Figure 1C. Pv^{TeNT}: n = 2 mice).
(E) Density of EDL sensory input to EDL motor neurons in p21 wild-type and p18 Pv^{TeNT} mice (WT: n = 14 MNs, as in Figure 1D. Pv^{TeNT}: n = 5 MNs).
(F) Density of EDL sensory input to TA motor neurons in p21 wild-type and p18 Pv^{TeNT} mice (WT: n = 18 MNs, as in Figure 1D. Pv^{TeNT}: n = 20 MNs).
(G and H) Distribution of EDL sensory boutons on soma and proximal ~100 μm dendrite of EDL motor neurons in p21 wild-type and p18 Pv^{TeNT} mice (wild-type as in Figure S1D and S1E. Pv^{TeNT}: n = 2 mice).
(I and J) Distribution of TA sensory boutons on soma and proximal ~100 μm dendrite of EDL motor neurons in p21 wild-type and p18 Pv^{TeNT} mice (wild-type as in Figure S1I and S1J. Pv^{TeNT}: n = 3 mice).
All data reported as mean ± SEM.

Supplemental Experimental Procedures

Estimation of Relative Homonymous and Heteronymous Connectivity Levels

We first determined the average percentage of vGluT1$^+$ boutons labeled by CTB across each homonymous synaptic pair for each motor neuron receiving input (indicated by red lines in Figure 1D). Because the degree of homonymous labeling varied across the three muscles, we computed the ratio between each homonymous pair (example: $\overline{TA \rightarrow TA} \div \overline{EDL \rightarrow EDL}$).

We then used the ratios to normalize our measurements of the average percentage of vGluT1$^+$ boutons labeled by CTB across each heteronymous synaptic pair. Example:

$\overline{EDL \rightarrow TA}_{n} = \overline{EDL \rightarrow TA} \times (\overline{TA \rightarrow TA} \div \overline{EDL \rightarrow EDL})$

Performing this normalization allowed us to compare the ratio of heteronymous to homonymous input onto each motor pool. Example:

Ratio of heteronymous to homonymous input on TA motor neurons = $\overline{EDL \rightarrow TA}_{n} \div \overline{TA \rightarrow TA}$

It also allowed us to estimate the relative contributions of homonymous and heteronymous input to the total input onto each motor pool. Example:

Percentage of homonymous input on TA = $\overline{TA \rightarrow TA} \div (\overline{TA \rightarrow TA} + \overline{EDL \rightarrow TA}_{n})$

Percentage of heteronymous input on TA = $(\overline{EDL \rightarrow TA}_{n}) \div (\overline{TA \rightarrow TA} + \overline{EDL \rightarrow TA}_{n})$

Spatial Analysis of Motor Pool Position

Individual motor neurons were assigned (x,y) coordinates with respect to the central canal in IMARIS and normalized to standard spinal cord dimensions: (1010, 640) at p21 and (760, 450) at p7. Contour plots in Figures 1B and 1D were generated from the normalized (x,y) coordinates. The centroid of each motor pool ($\overline{x}$,$\overline{y}$) was calculated by averaging the normalized x and y coordinates across all motor neurons within the pool. The position of each motor neuron with respect to the centroid of a neighboring motor pool was determined as ((x-$\overline{x}$),(y-$\overline{y}$)) for each motor neuron within a pool. These Cartesian coordinates were then converted to polar coordinates in order to generate the polar plots shown in Figure S3.

Whole Cell Recordings from Visually-Identified Motor Neurons in a Spinal-Hindlimb Preparation

P0 pups were injected with CTB-488 in either TA or PL muscles. At day of physiological experiment, p2-p6 animals were decapitated and the spinal cord dissected and removed under cold (~9°C) artificial cerebrospinal fluid (aCSF) containing in mM: 128.35 NaCl, 4 KCl, 0.58 $NaH_2PO_4.H_20$, 21 $NaHCO_3$, 30 D-Glucose, 1.5 $CaCl_2.H_20$, and 1 $MgSO_4.7H_20$. The spinal cord was dissected in continuity with the sciatic nerve and hind limb. The L4 and L5 ventral roots were cut, leaving intact the dorsal roots. The sural and tibial nerves were cut close to the entry point of the hind limb leaving the common peroneal nerve intact, which innervates the TA, EDL and PL muscles. The spinal cord-hind limb preparation was then transferred to a customized recording chamber located under the objective of a confocal microscope (Leica SP5) equipped with 3 single photon (488, 543, 633nm) and a 2-photon laser (Spectra Physics, Mai Tai Deep See), and perfused continuously with oxygenated (95%O_2/5%CO_2) aCSF (~13 ml/min). Ventral roots were placed into suction electrodes to stimulate motor neuron axons. Concentric needle electrodes (P12CEA3, Microprobes, MD, USA) were inserted into the belly of the TA, EDL and PL muscles to activate proprioceptive fibers from each muscle.

Whole-cell recordings were obtained with patch electrodes advanced through the lateral aspect of the intact spinal cord. The electrodes were filled with intracellular solution containing (in mM): 10 NaCl, 130 K-Gluconate, 10 HEPES, 11 EGTA, 1 $MgCl_2$, 0.1 $CaCl_2$ and 1 Na_2ATP, pH adjusted to 7.2–7.3 with KOH. Alexa 543 Hydrazide (50 µM) was added to the solution to label the recorded motor neuron (final osmolarity of the intracellular solution was ~305–309 mOsm).

Motor neurons were visually targeted after removal of the dura and pia mater from the lateral aspect of the cord over the L3-L6 spinal segments. By pre-labeling TA and PL motor neurons *in vivo*, we were able to cut the ventral roots and thereby avoid using antidromic stimulation of a muscle to determine the identity of motor neurons. Muscle stimulation results in an antidromic action potential in the homonymous motor neuron and the disynaptic recurrent IPSP (Mentis et al., 2005), which would have complicated detection of the afferent-evoked EPSPs. The patch electrode was controlled by a motorized four-axis micromanipulator (Scientifica, UK) and was advanced towards the motor neuron nucleus. The identity of the recorded neuron was initially confirmed as a motor neuron by the presence of an antidromic action potential following ventral root

stimulation. Single or two-photon excitation (when depth of pool > 70 μm) was used to confirm the muscle identity of the motor neuron recorded by checking for co-localization of CTB-488 with the intracellular solution containing Alexa 543 Hydrazide.

Motor neurons were accepted for further analysis only if the following three criteria were met: (i) resting membrane potential of −50mV or more negative (ii) an overshooting antidromically evoked action potential and (iii) at least 30 minutes of recording. All measurements of synaptic potentials were made at −60mV using continuous current injection if necessary. Synaptic potentials were recorded from individual motor neurons (DC - 3 KHz, Multiclamp 700A, Molecular Devices) in response to stimulation of each of the three muscles (A365, current stimulus isolator, WPI, FL). The stimulus threshold was defined as the stimulation current at which the minimal evoked response was recorded in 3 out of 5 trials at 0.2 Hz. The muscles were stimulated at 2x and 5x threshold resulting in suprathreshold (or maximal) responses. Recordings were fed to an A/D interface (Digidata 1320A, Molecular Devices) and acquired with Clampex (v9, Molecular Devices) at a sampling rate of 10 KHz. Data were analyzed offline using Clampfit (Molecular Devices). Measurements were made on averaged traces (3–10 trials).

Extracellular Ventral Root Recordings Following Dorsal Root Stimulation

Following spinal cord isolation in oxygenated aCSF, suction electrodes were placed in the L4 and L5 dorsal and ventral roots. Extracellular recordings (Cyberamp, Molecular Devices; amplified 1000x and acquired at DC - 3 KHz) were obtained from L4 and L5 ventral roots in response to stimuli (duration 0.2 ms) from the dorsal roots (L4 or L5) delivered by a stimulus isolator (A365 - WPI, Sarasota, FL) at 2-5x threshold. Extracellular recordings were sampled at 10 KHz and the recordings were analyzed off-line using Clampfit (Molecular Devices). Off-line analysis was performed by averaging 3 to 10 traces. The latency of the afferent-evoked ventral root potentials was defined as the time from the onset of the stimulus artifact to the first measurable deflection of the potential from the baseline.

Whole Cell Recordings from Individual Motor Neurons Following Dorsal Root Stimulation

In intracellular recordings, synaptic potentials were recorded from individual motor neurons (DC - 3 KHz, Multiclamp 700A, Molecular Devices) in response to orthodromic stimulation (A365, current stimulus isolator, WPI, Sarasota, FL) of a dorsal root (L4 or L5). Motor neurons were

patched blindly. Motor neuron identity was confirmed by the presence of antidromic evoked action potential following ventral root stimulation. The stimulus threshold was defined as the current at which the minimal evoked response was recorded in 3 out of 5 trials. The nerve was stimulated at 2-5x threshold. Recordings were fed to an A/D interface (Digidata 1320A, Molecular Devices) and acquired with Clampex (v9, Molecular Devices) at a sampling rate of 10 KHz. Data were analyzed off-line using Clampfit (Molecular Devices). Measurements were made on averaged traces (3-10 trials).

Supplemental References

Bácskai, T., Rusznák, Z., Paxinos, G., and Watson, C. (2014). Musculotopic organization of the motor neurons supplying the mouse hindlimb muscles: a quantitative study using Fluoro-Gold retrograde tracing. Brain Struct. Funct. *219*, 303–321.

McHanwell, S., and Biscoe, T.J. (1981). The Localization of Motoneurons Supplying the Hindlimb Muscles of the Mouse. Philos. Trans. R. Soc. B Biol. Sci. *293*, 477–508.